Ahmed Kasdi[1,*], Youcef Zebboudj[1], Hakim Yala[2]

J. Electrical Systems 11-4 (2015): 384-396

Regular paper

Simulation of Corona Discharge in DC Electrostatic Precipitator

The stable positive DC corona discharge in atmospheric air under a wire-to-cylinder system is analyzed in this paper. An iterative finite element technique is developed to obtain a general solution of the governing equations of the coupled space-charge and electric field problem. The technique is to use the finite-element method (FEM) to solve Poisson s equation and the method of characteristics (MOC) to find the charge density from a current-continuity relation. Besides, the corona ionized field is successfully modeled using COMSOL MULTIPHYSICS 3.4. Two application modes are used to solve system of coupled equations with appropriate boundary conditions: PDE (General Form) mode for electric potential distribution and Convection and Diffusion mode for charge transport equation. In order to validate the presented numerical methods a comparison with analytical solution and measured data are made. The obtained results are in good agreement.

Keywords: Electrostatic Precipitator, corona discharge, space charge, finite element method, ionized field.

Article history: Received 6 July 2015, Received in revised form 14 October 2015, Accepted 1 November 2015

1. Introduction

Corona discharge is currently used in various ways in an increasing number of industrial and technological applications, such as electrostatic precipitator (ESP) and separators, ozonizers, painting and spraying powders, etc. Moreover, it has been the subject of many theoretical, experimental and numerical studies in diverse gaps configurations [1-16]. In this paper, we are interested about the numerical modeling of a coaxial ESP for which the configuration is symmetric with stable corona discharge.

The principle of electrostatic precipitator that use corona discharge phenomenon can be described as following. A high intensity electric field is applied between a high tip curvature corona electrode (wire) and a low tip curvature collector electrode (cylinder) provides condition for ionization of gas molecules in the nearest vicinity of corona electrode surface. The inter-electrode space is divided in two distinct regions; a high-field ionization region surrounded the active electrode where free charges are produced, and a low-field drift region occupying the remainder of the interval. In the case of positive corona, the electrons move toward corona electrode and are neutralized whereas positive ions are pushed by the electric field away from it and drift to the passive collector electrode forming a space charge which modifies the original Laplacian applied electric field.

Despite advances in numerical and computational techniques, accurate solutions of the field equations are very difficult to obtain because of the distortion of the electric field due to the presence of the space charge. Several numerical techniques have therefore been employed to solve the problem using the charge simulation method [1-2], the finite difference method [3] and the finite element method [4-8], often combined with the method of characteristics [7,9-11] to evaluate the space charge density. The study of a symmetric

* Corresponding author: A. Kasdi, Electrical Engineering Laboratory, University of Bejaia, 06000 Bejaia, Algeria, E-mail: ahmed.kasdi@univ-bejaia.dz
[1] Faculty of Technology, University of Bejaia, 06000 Bejaia, Algeria
[2] Faculty of Exact Sciences, University of Bejaia, 06000 Bejaia, Algeria

coaxial system for which an analytic solution is available will allow to modeling other complex geometries.

2. Mathematical model

In the air, the mathematical description of the monopolar ionized field is giving by this set of equations:

Poisson's equation:

$$\nabla.\vec{E} = \rho/\varepsilon_0 \tag{1}$$

Equation for current density:

$$\vec{J} = \mu.\rho.\vec{E} - D.\nabla\rho \tag{2}$$

Equation for current continuity:

$$\nabla.\vec{J} = 0 \tag{3}$$

Equation relating the field to the potential:

$$\vec{E} = -\nabla\Phi \tag{4}$$

Where $\vec{E}$ is the electric field, ϕ the electric potential, $\vec{J}$ the current density vector, ρ the ionic charge density, ε_0 the air permittivity, μ the ionic mobility, and D the diffusion coefficient.

Because of its nonlinear character, equations (1)-(4) cannot be solved analytically except for very simple geometries (infinite parallel plates, concentric spheres, etc.). Therefore, all numeric methods proposed in the literature to resolve the corona problem in practical line geometries have resorted to some simplifying assumptions [4-8], where the most common ones are:

- The thickness of the active ionization layer around the wire is so small as to be neglected with respect to the inter-electrode spacing [10].
- The average mobility μ of positive ions is assumed constant (independent of electric field intensity) during the transit time from the ionization region to the collecting electrode [12-14].
- For applied voltages above corona onset level, the field on the wire surface remains constant at the threshold field E_i, independently of the corona intensity (Kaptzov's assumption) [15].
- Diffusion of ions is neglected in comparison with migration [10].

Solution of the equations (1)-(4) should be supplemented with these proper boundary conditions:

- The potential on the coronating wire is equal to the applied voltage ($\phi_w = V_a$).
- The potential on the grounded electrode (cylinder) is zero ($\phi_C = 0$);

- The magnitude of the electric field at the surface of the coronating wire remains constant at the threshold field E_i. This value, often given by the empirical Peek's law [15], is replaced in the present paper by the generalized Peek's law developed in [12]. The threshold field E_i normalized at the related air density is expressed by this analytic equation [14]:

$$E_i(R,\delta,H_a) = E_c(1,0)\times\delta\times F(H_a,\delta,R) \tag{5}$$

Where $E_c(1,0) = 2.468\times10^6$ V/m is the minimum ionization field corresponding to the effective ionization coefficient $\alpha-\eta = 0$. $F(H_a,\delta, R)$ is a function depending on the radius R of the wire, on the absolute humidity H_a and on the related air density δ.

This boundary condition is satisfied by adjusting iteratively the charge density ρ_w on the wire surface until the electric field at the wire agrees with the threshold field value [4].

3. Proposed method of analysis

In the present investigation, the wire cylinder system is supposed to be of infinite length and consequently the system is reduced to a two-dimensional (2D) system. A wire of radius R_W forms the anode and a cylinder of radius R_C forms the cathode as indicated in Figure 1.

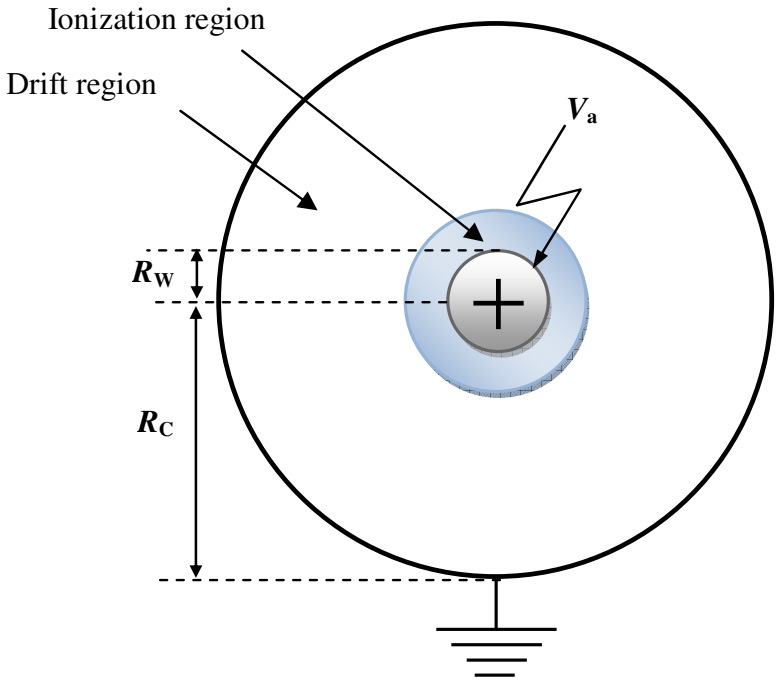

Figure 1. DC corona structure representation in coaxial system

Corona governing equations, seen previously, clearly indicate the physical interactions between electric field E and space charge density ρ. The process of numerical calculations is therefore, iterative by nature. In the calculation process proposed, unknown space functions, i.e. electric potential and positive ion density were evaluated alternatively, from the coupled differential equations, assuming that the second quantity was known from the

previous iteration steps. A first order triangular finite element with a constant ionic charge density in each element is adopted.

3.1 Resolution of Poisson's equation

The finite element method approximates the potential within each element as a linear function of coordinates:

$$\phi^e(x, y) = a^e + b^e x + c^e y \tag{6}$$

For known values of ρ at nodes, Poisson's equation (1) is solved by minimizing an energy functional with respect to each nodal potential value. This minimization leads to a set of simultaneous equations for values of ϕ at nodes. The electric field within any particular element is constant and given by:

$$\vec{E} = -b^e \vec{i_x} - c^e \vec{i_y} \tag{7}$$

3.2 Evaluation of the space charge density

The space charge distribution in the computational domain is obtained by applying the method of characteristics (MOC) to solve the continuity equation (3), where ion diffusion is neglected. This method introduces the time as a new variable to evaluate the space charge density along field lines [10].

Under the effect of the electric field, the positive ions acquire the speed:

$$\vec{v} = \mu \vec{E} \tag{8}$$

Ion trajectories are then defined by:

$$\frac{d\vec{r}}{dt} = \mu . \vec{E} \tag{9}$$

Where *r* is the rectilinear coordinate measured along the field line.

Combining the equations (1)-(3), one obtains a non linear partial differential equation governing the evolution of the space charge density:

$$\vec{E} . \vec{\nabla} \rho = -\frac{\rho^2}{\varepsilon_0} \tag{10}$$

Equation (10) can be written, along the characteristic field line, as:

$$\frac{d\rho}{dt} = -\mu \frac{\rho^2}{\varepsilon_0} \tag{11}$$

This equation yields an analytical solution of the following form:

$$\rho(t) = \left(\frac{\mu.t}{\varepsilon_0} + \frac{1}{\rho_0} \right)^{-1} \tag{12}$$

where ρ_0 is the charge density at the starting point of the characteristic line.

Ion trajectories in the coaxial configuration are straights and radial to the wire. So, given the known electric field on each grid node, equation (9) is used to determine the time-step Δt corresponding to an increment distance Δr along the field line. The value of time is then replaced in equation (12) to find the space charge density.

4. Procedure of resolution

The method of analysis is described in the following steps:

- *Step* (1)*:* Orthogonal grid generation: The area is divided in to triangular elements forming a grid which is generated by the intersection of N_r equally spaced radial lines with N_c concentric circular contours. The points of intersection represent the grid nodes and the simple triangular finite elements are obtained by subdividing each quadrangle into two triangles [11]. The radial distance between nodes is small near the coronating conductor and increases in the direction towards the outer conductor.

- *Step* (2): Solve for ϕ via the finite element method the Laplace's equation ($\nabla^2\phi$ = 0) assuming ρ= 0 in the entire domain.

- *Step* (3): Make an initial guess for ρ_w, the space charge density on the wire surface.

- *Step* (4): Calculate the electric field distribution from the potential interpolation.

- *Step* (5): Apply the MOC to obtain the charge density at grid nodes.

- *Step* (6): Using FEM, solve for the potential ϕ the Poisson's equation with the new charge density.

- *Step* (7): Repeat steps (4)-(6) until the maximum mismatch between the two last estimates of the potential at the grid nodes is less than a pre-specified error δ_1.

- *Step* (8): Calculate the electric field magnitude at the wire's surface and compare it to the threshold field value, E_i.
  - If sufficiently close (with respect to a pre-specified error δ_2), stop.
  - Else, correct the space charge density ρ_w at the wire and return to step (4).

We summarize in Figure 2 the flowchart of the FEM-MOC simulation program.

5. Results and discussion

The described method was tested through its application to a 30 kV ESP laboratory model, for which experimental results are available [14]. The computational model consists of a wire of radius R_W=0.9875 mm and a cylinder of radius R_C = 50 mm for which the

corona threshold field value E_i is evaluated at 6.06 MV/m and the corona onset voltage V_{ons} is 23.48 kV. The ionic mobility is μ= 2.15 10^{-4} m^2/Vs and the errors δ_1 (on electric potential) and δ_2 (on electric field) were taken 1 %.

An example of the finite-element mesh that covers the area of interest around the coronating wire is shown in Figure 3. In the area close to the corona wire, where high gradient is expected, the mesh has a high concentration while elsewhere the elements can be larger. The generated mesh is formed by 950 triangular elements and 500 nodes.

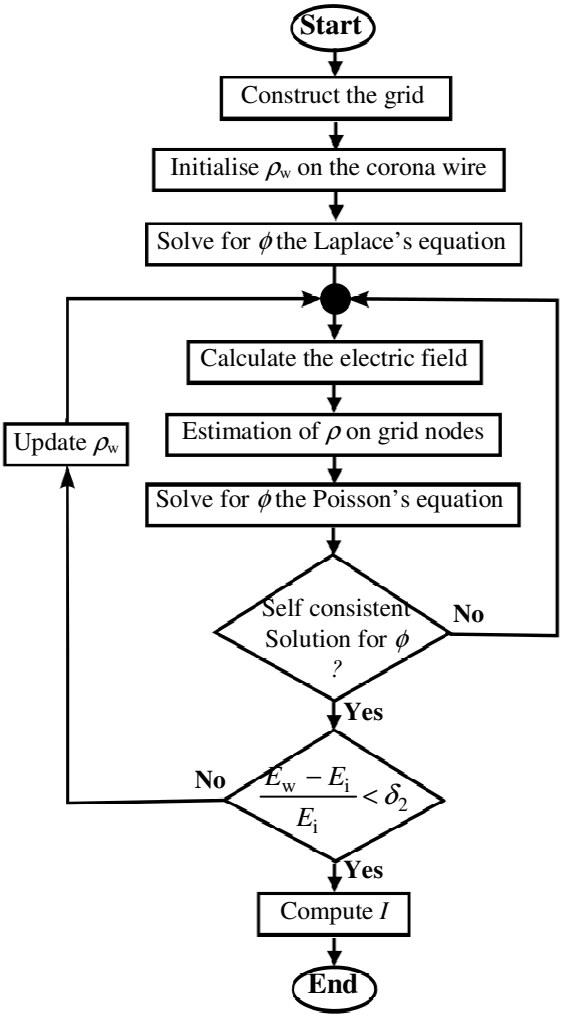

Figure 2. Chart flow of the numerical procedure

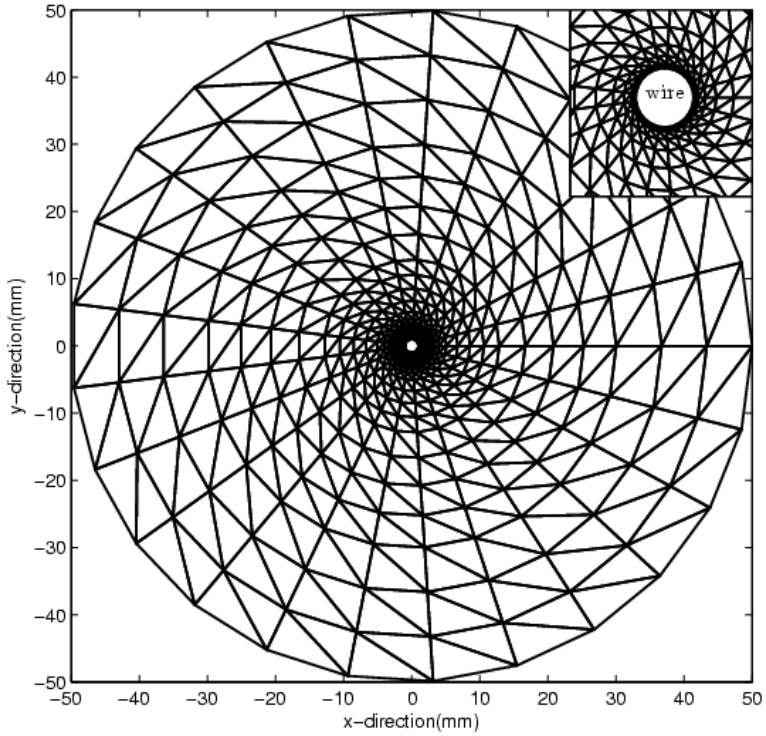

Figure 3. Generated grid for a wire-cylinder system

5.1 Current– voltage characteristics

A corona discharge can be characterized globally by the current-voltage curve which relates the current collected by the outer cylinder to the voltage applied to the wire. The corona current can be computed by integrating the current density over the round cylinder (or wire) surface. At a given value of the applied voltage V_a, the current I per unit length is given by :

$$I = \iint_S J.dS = 2\pi R_w \times (\mu.\rho_w E_w) \tag{13}$$

where ρ_w and E_w are the charge density and the electric field values at the corona wire respectively.

Figure 4 shows the current-voltage characteristic curves for the investigated coaxial system configuration. The current is negligible until voltage is equal to the onset value. Starting from that point, the current increases rapidly with the applied voltage. As can be seen, the characteristics predicted by both FEM-MOC technique and Comsol model are very close and agree well with the measured curve giving by [14].

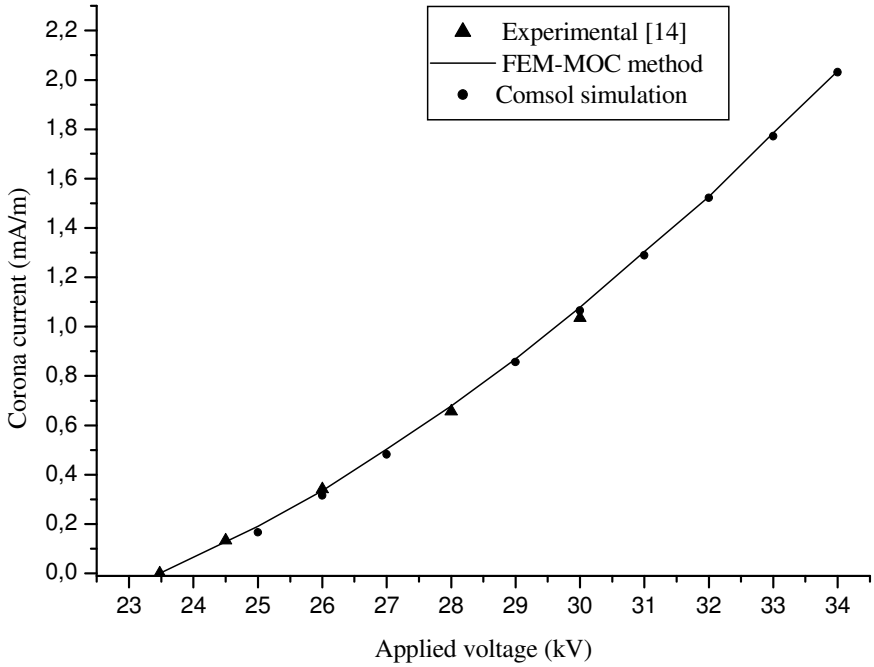

Figure 4. Current-Voltage characteristics for the investigated coaxial system

5.2 Space charge effect on electric field distribution

The calculated Poissonian and Laplacian electric field distributions along the radial direction are shown in Figure 5. The Poissonian field in the ionization region is lower and remains constant at the wire surface as it results from Peek's assumption. On the other hand, the concentration of positive ions near the ground cylinder increases the total electric field with regard to Laplacian free-field. It is clear that the presence of space charge in the gap has a significant effect on the electric field, consistent with previous studies [11,14].

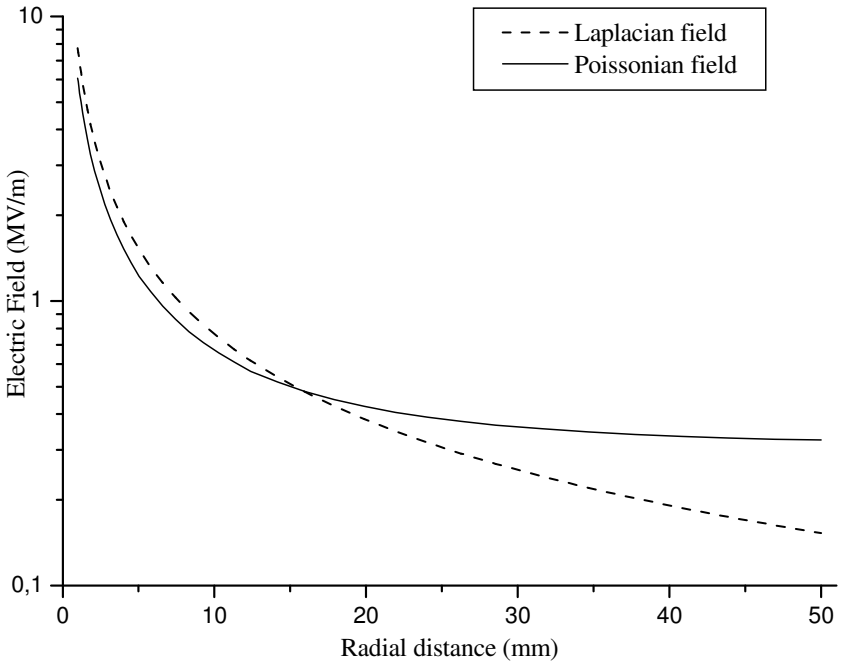

Figure 5. Poissonian and Laplacian electric field distributions along the radial direction

5.3 Electric field, electric potential and space charge distributions

The computational distributions of the electric field, the electric potential and the space charge density along the radial direction are shown in Figures 6, 7 and 8 respectively, and compared with the semi-empirical solution given by [4,14]. It can be seen that the electric field intensity around the corona wire is very strong and declines according to a $1/r$ law near the ionization region. For a high value of r, the electric field decreases slightly and becomes constant when r is close to R_C. Similarly, the electric potential is very important in the ionization region where it takes the maximum value of V_a, the applied voltage, at $r = R_w$, becomes low away from the wire and reaches zero at the cylinder surface, as the cylinder is grounded. The space charge is also distributed with highest density near the wire and decreasing away from it. In all cases, the calculated values predicted by the two presented models (FEM-MOC technique and Comsol simulation) are in good agreement with those given by the analytic solution.

Comsol Multiphysics software has the ability to represent the calculated results in several graphical presentations, among others, the presentation with colors [17]. Figures 9 to 11 show the two-dimensional computed distributions of the electric field, the electric potential and the space charge density, respectively, together with the coordinate directions where the centre of the corona wire is taken as the origin. As previously seen, the corona discharge parameters have high values at the wire surface and low values at the grounded cylinder. The magnitudes of calculated values are demonstrated by scale of colors. Also, a number of field lines and equipotential contours are traced in white in Figure 09 and Figure 10, respectively. It is seen that the field lines are straight and radial and the potential contours are concentric circles around the corona wire due to the revolution symmetry of the system.

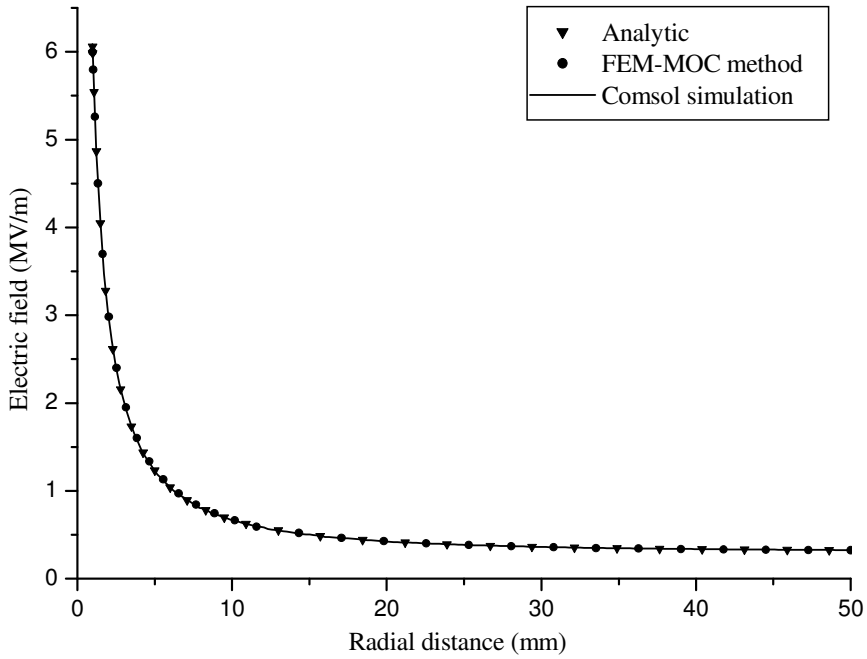

Figure 6. Electric field distribution along the radial direction

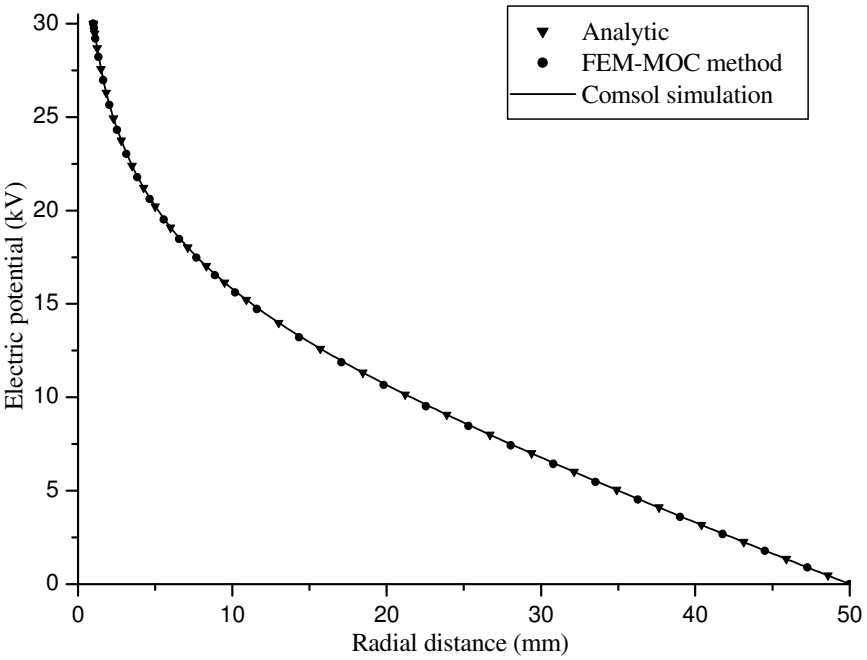

Figure 7. Electric potential distribution along the radial direction

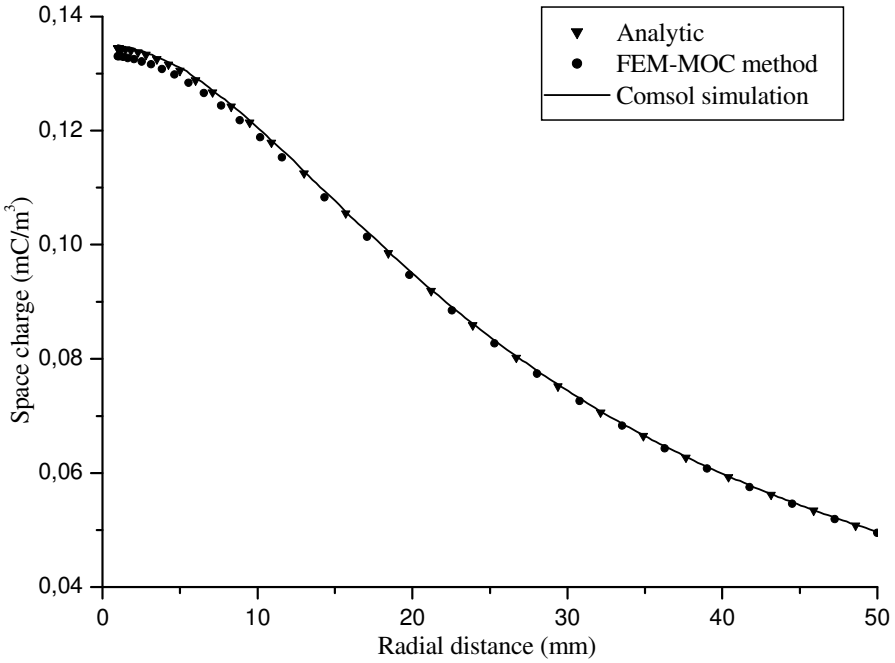

Figure 8. Space charge density distribution along the radial direction

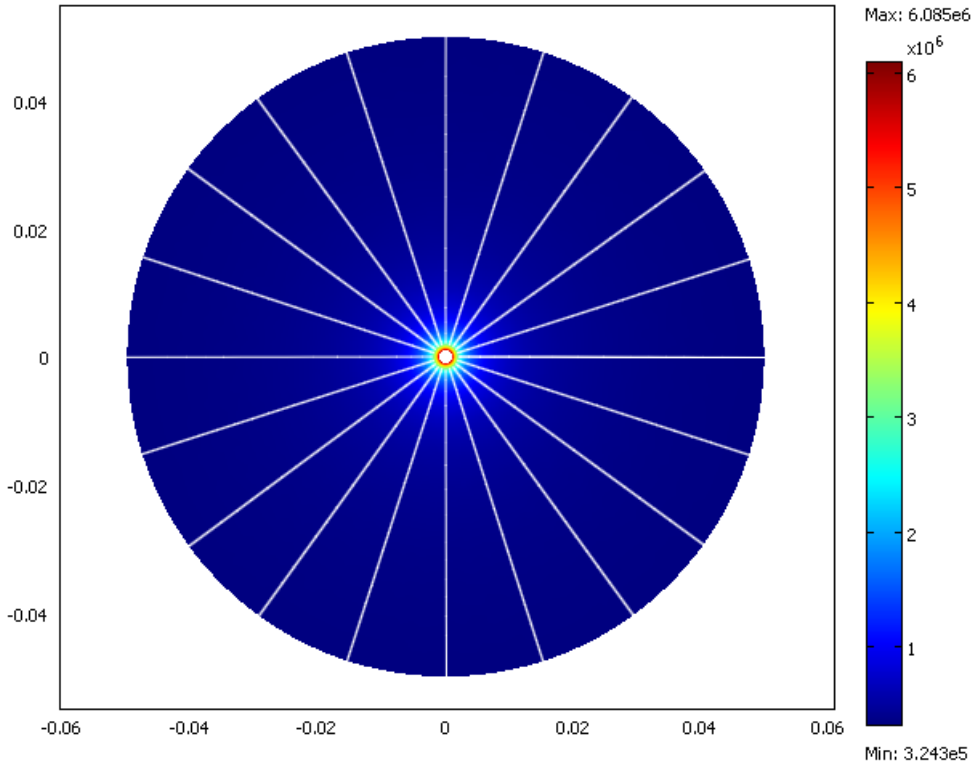

Figure 9. 2D electric field distribution in the computed domain

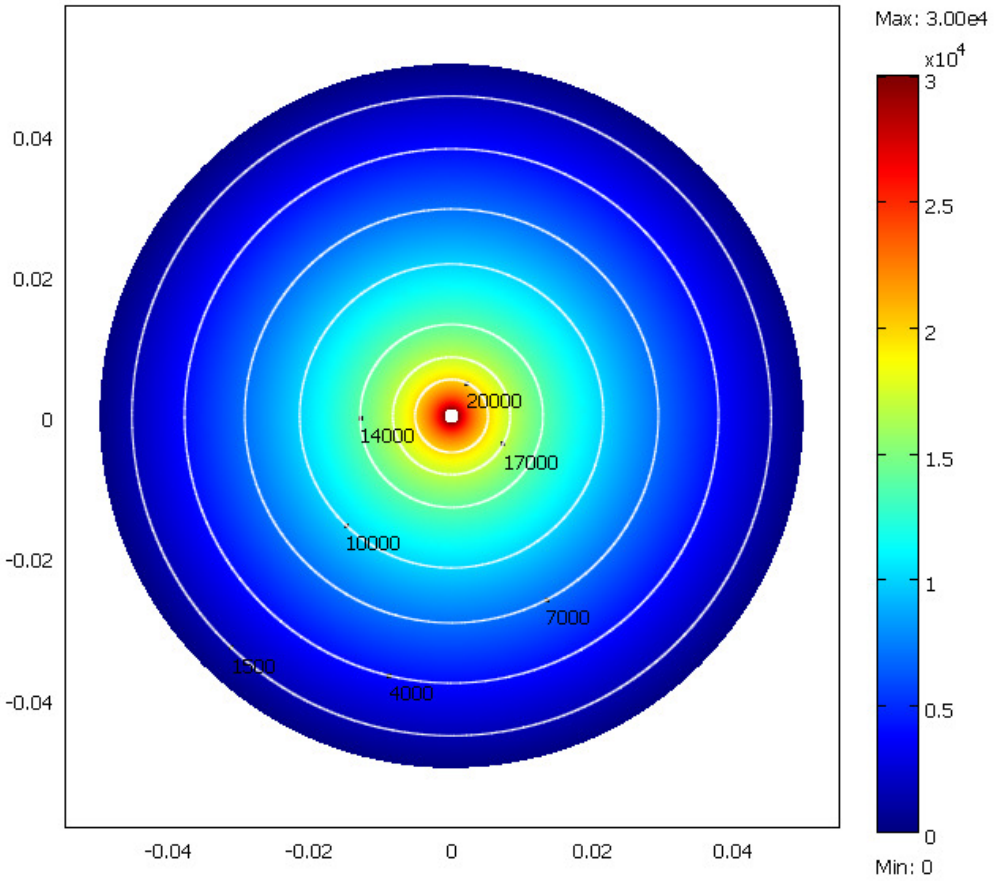

Figure 10. 2D electric potential distribution in the computed domain

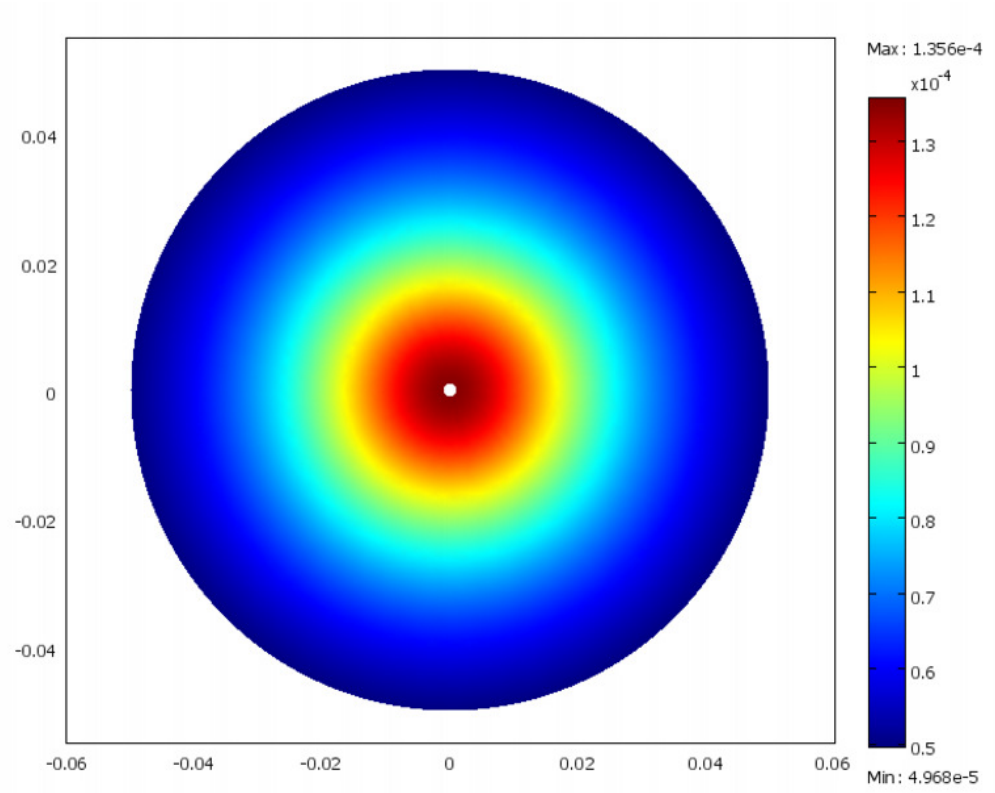

Figure 11. 2D space-charge density distribution in the computed domain

6. Conclusion

The present study has developed an efficient iterative method for the solution of the ionized field problem during the positive DC corona discharge in coaxial system. Thereafter, the corona governing equations are implemented and solved effectively using COMSOL Multiphysics software. Predictions of both numerical models are with good agreement with the analytic solution and the experimental data. The Comsol program is fairly simple and very quickly with high precision. The successful application of Comsol Multiphysics to simulate the corona discharge in a coaxial geometry have recently allowed us to model more complex geometries, such as a wire-plate and a multi-wires-plate configurations. Other electrode systems are being investigated.

References

[1] M. Horenstein, Computation of corona space charge, electric field, and V-I characteristic using equipotential charge shells, *IEEE Trans. Ind. Appl. 20*, 1607-1612, 1984.
[2] A.A. Elmoursi, G.S. Peter Castle, The analysis of corona quenching in cylindrical precipitators using charge simulation, *IEEE Trans. Ind. Appl. 22*, 80-85, 1986.
[3] C. Budd, Coronas and the space charge problem, Euro. J. Appl. Math. 2, 43-81, 1991.
[4] W. Janischewskyj, G. Gela, Finite element solution for electric fields of coronating DC transmission lines, *IEEE Trans. Power Appl. And Syst. 98*, 1000-1012, 1979.
[5] Z. M. Al-Hamouz, A. El-Hamouz, N Abuzaid, Simulation and experimental studies of corona power loss in a dust loaded wire-duct electrostatic precipitator, *Advanced Powder Technology 22*, 706-714, 2011.
[6] S. Cristina, G. Dineli, M. Feliziani, Numerical computation of corona space charge and V-I characteristic in DC electrostatic precipitators, *IEEE Trans. Ind. Appl. 27*, 147-153, 1991.
[7] Z. M. Al-Hamouz, Numerical and experimental evaluation of fly ash collection efficiency in electrostatic precipitators, *Energy Conversion and Management 79*, 487–497, 2014.
[8] M. Abdel-Salam, Z.M. Al-Hamouz, A new finite-element analysis of an ionized field in coaxial cylindrical geometry, *J. Phys. D: Appl. Phys. 25*, 1551-1555, 1992.
[9] J. Anagnostopoulos, G. Bergeles, Corona discharge simulation in wire-duct electrostatic precipitator, *Journal of Electrostatics 54*, 129-147, 2002.
[10] L. Zhao, K. Adamiak, Numerical Simulation of the Effect of EHD Flow on Corona Discharge in Compressed Air, *IEEE Trans. Ind. Appl. 49*, 298-304, 2013.
[11] A. Kasdi, Y. Zebboudj, H. Yala, Calculation and measurement of electric field under HVDC transmission lines, *EPJ-Applied Physics 37*, 323-329, 2007.
[12] G. Hartmann, Theoretical evaluation of Peek law. *IEEE Trans, Ind. Appl. 20*, 1647-1651, 1984.
[13] J.E. Jones, J. Dupuy, G.O.S. Schreiber, R.T. Waters, Boundary conditions for the positive direct-current corona in coaxial system, *J. Phys. D, Appl. Phys. 21*, 322-333, 1988.
[14] Y. Zebboudj, G. Hartmann, Current and electric field measurements in coaxial system during the positive DC corona in humid air, *EPJ-Applied Physics 7*, 167-176, 1999.
[15] N.A. Kaptzov, Elektricheskie Invlentiia v Gazakh i Vakuumme, *OGIZ Moscow (URSS)*, 587-630, 1947.
[16] F.W. Peek, Dielectric phenomena in H.V. engineering, *McGraw Hill*, 52-80, 1929.
[17] COMSOL MULTIPHYSICS 3.4 – User's guide –, documentation 2007.